

Numerical study of metastability due to tunneling: The quantum string method

Tiezheng Qian

*Department of Mathematics, Hong Kong University of Science and Technology,
Clear Water Bay, Kowloon, Hong Kong, China*

Weiqing Ren

*Department of Mathematics, Princeton University,
Princeton, New Jersey 08544, USA*

Jing Shi

*Program in Applied and Computational Mathematics, Princeton University,
Princeton, New Jersey 08544, USA*

Weinan E

*Department of Mathematics and PACM, Princeton University,
Princeton, New Jersey 08544, USA*

Ping Sheng

*Department of Physics and Institute of Nano Science and Technology,
Hong Kong University of Science and Technology, Clear Water Bay, Kowloon, Hong Kong, China*

We generalize the string method, originally designed for the study of thermally activated rare events, to the calculation of quantum tunneling rates. This generalization is based on the analogy between quantum mechanics and statistical mechanics in the path-integral formalism. The quantum string method first locates, in the space of imaginary-time trajectories, the minimal action path (MAP) between two minima of the imaginary-time action. From the MAP, the saddle-point (“bounce”) action associated with the exponential barrier penetration probability is obtained and the pre-exponential factor (the ratio of determinants) for the tunneling rate evaluated using stochastic simulation. The quantum string method is implemented to calculate the zero-temperature escape rates for the metastable zero-voltage states in the current-biased Josephson tunnel junction model. In the regime close to the critical bias current, direct comparison of the numerical and analytical results yields good agreement. Our calculations indicate that for the nanojunctions encountered in many experiments today, the (absolute) escape rates should be measurable at bias current much below the critical current.

PACS numbers: 74.50.+r, 74.20.De, 82.20.Wt, 05.10.-a

I. INTRODUCTION

One of the most important problems in statistical physics involves the rate of decay of a system rendered unstable by thermally activated barrier crossing [1–3] and/or quantum barrier tunneling [4–6], and functional integrals represent a fundamental tool for studying these transition processes. However, numerical evaluation of the functional integrals has always been a challenge. Recently, the string method has been proposed for the numerical evaluation of thermally activated rare events [7–11]. This method first locates the most probable transition pathway connecting two metastable states in configuration space. The transition rates can then be computed by numerically evaluating the fluctuations around the most probable pathway.

The purpose of this paper is to generalize the string method to the study of quantum metastability caused by barrier tunneling. The theory of the decay rate through barrier tunneling has been formulated using the imaginary-time functional integral techniques [4]. Essentially, the saddle point of the imaginary-time action is first located and the rate of decay is then obtained by evaluating the relevant fluctuations. Within the functional integral formalism, the computational task for a quantum field in d -dimensional space is equivalent to that for a classical field in $(d+1)$ -dimensional space [4]. Therefore, the quantum version of the string method can be numerically implemented as its original classical version for a higher dimensional system.

It should be noted that while in zero-dimensional tunneling problems (a quantum particle is regarded as a zero-dimensional quantum field, as in the example presented below) the quantum string method might not offer any special advantage than, e.g., the well-known WKB method, in higher dimensional problems or in field theoretical formulations, the usual wave-mechanics approach becomes very difficult to implement. It is precisely in such problems that the present approach can offer an efficient numerical tool in finding the path of “least action”, and on that basis calculate the relevant tunneling rate(s).

The paper is organized as follows. In Sec. II we outline the string method for the numerical evaluation of thermal activation rate and generalize it to the evaluation of quantum tunneling rate. In Sec. III we apply the quantum string method to study the current-biased Josephson junction [12–15]. This physical model has long been used to demonstrate the quantum mechanical behavior of a single macroscopic degree of freedom (the phase difference across the tunnel junction) [15]. It has also played an important role in the study of macroscopic quantum tunneling [16]. The escape rate of the junction from its zero-voltage state is numerically evaluated at zero temperature in the absence of dissipation. For bias currents less than but very close to the critical current, the tilted-washboard potential can be approximated by the quadratic-plus-cubic potential, for which the analytic form of the quantum tunneling rate has been obtained [17,18]. Our numerical results obtained for this “solvable” model show good agreement with the previous analytic results, and thus affirm the validity of the quantum string method. In Sec. IV we conclude the paper with a few remarks on the relationship of our results to quantum dissipation.

II. QUANTUM STRING METHOD

A. String method for thermally activated rare events

The string method was originally presented for the numerical study of thermal activation of metastable states [7]. Consider a system governed by the energy potential $V(\mathbf{q})$ in the overdamped regime, where \mathbf{q} denotes the generalized coordinates $\{q_i\}$. The minima of $V(\mathbf{q})$ in the configuration space correspond to the metastable and stable states of the system. Given \mathbf{q}_A and \mathbf{q}_C as the two minima of V , the most probable fluctuation which can carry the system from \mathbf{q}_A to \mathbf{q}_C (or \mathbf{q}_C to \mathbf{q}_A) corresponds to the lowest intervening saddle point \mathbf{q}_B between these two minima, with the transition rate given by [1–3]

$$\Gamma_T(A \rightarrow C) = \frac{|\lambda_B|}{2\pi\eta} \left[\frac{|\det H(\mathbf{q}_B)|}{|\det H(\mathbf{q}_A)|} \right]^{-1/2} \exp \left\{ -\frac{\Delta V}{k_B T} \right\}, \quad (1)$$

where η is the frictional coefficient, $H(\mathbf{q})$ denotes the Hessian of $V(\mathbf{q})$, λ_B is the negative eigenvalue of $H(\mathbf{q}_B)$, and $\Delta V = V(\mathbf{q}_B) - V(\mathbf{q}_A)$ is the energy barrier. For the numerical evaluation of Γ_T , we define the minimal energy path (MEP) as a smooth curve $\mathbf{q}^*(s)$ in configuration space. It connects \mathbf{q}_A and \mathbf{q}_C with intrinsic parametrization such as arc length s , satisfying

$$(\nabla V)^\perp(\mathbf{q}^*) = 0, \quad (2)$$

where $(\nabla V)^\perp$ is the component of ∇V normal to the curve $\mathbf{q}^*(s)$. Physically, the MEP is the most probable pathway for thermally activated transitions between \mathbf{q}_A and \mathbf{q}_C . To numerically locate the MEP in \mathbf{q} space, a string $\mathbf{q}(s, t)$ (a smooth curve with intrinsic parametrization by s) connecting \mathbf{q}_A and \mathbf{q}_C is evolved according to

$$\left(\frac{d\mathbf{q}}{dt} \right)^\perp = -(\nabla V)^\perp(\mathbf{q}), \quad (3)$$

where $(d\mathbf{q}/dt)^\perp$ denotes the velocity normal to the string [7]. To enforce the desired parametrization, e.g., equal arc length, the string is reparametrized every a few time steps. The stationary solution of Eq. (3) satisfies Eq. (2) which defines the MEP. Once the MEP is determined, the intervening saddle point \mathbf{q}_B is known. The negative eigenvalue λ_B and the corresponding eigenvector can be directly obtained from the MEP, and the ratio of the determinants in Eq. (1) can be numerically computed using a stochastic method [9].

The above scheme for the calculation of thermal activation rates has many applications, e.g., the condensation of a supersaturated vapor, the realignment of a magnetic domain [7,8], and the decay of persistent current in one-dimensional superconductor [19,20,11]. All of these transition processes occur when the system undergoes a fluctuation that is large enough to initiate the transition. Physically, the thermal activation rate Γ_T becomes practically unmeasurable as the temperature is sufficiently low ($k_B T \ll \Delta V$). However, even though thermodynamic fluctuations are

suppressed at low temperatures, a system can still be rendered unstable by quantum barrier tunneling [4]. The simplest example is a particle that escapes a potential well: it penetrates a potential barrier and emerges at the escape point with zero kinetic energy, after which it propagates classically. In quantum field theory, a classical false vacuum is rendered unstable by bubbles of the true vacuum, realized through tunneling. Once these bubbles are sufficiently large, they become energetically favorable to grow.

B. Rate of barrier tunneling

The theory for the rate of barrier tunneling has been formulated [4] and generalized [5,6] using the imaginary-time functional integral techniques. Here we show that the string method can be generalized to be an efficient numerical tool (the quantum string method) for the calculation of tunneling rates. In order to make concrete the formulation of the approach, below we consider a quantum particle that escapes a potential well through barrier tunneling. This zero-dimensional case can be extended to a quantum field, where the classical false vacuum is rendered unstable by barrier tunneling [4]. These results show that for a quantum field in d -dimensional space, the computational task may be reduced to the calculation of thermodynamic transition rates for a classical field in $(d+1)$ -dimensional space.

Consider a particle of mass m moving in a one-dimensional potential $U(q)$ with two minima q_0 and q_1 , one of which, q_1 , is the absolute minimum (see Fig. 1a). Assume $U(q_0) = 0$ and q_1 is to the right of q_0 ($q_1 > q_0$). The normalized harmonic-oscillator ground state $\psi_g(q)$, centered at q_0 , is $\psi_g(q) = (m\omega_0/\pi\hbar)^{1/4} \exp[-m\omega_0(q - q_0)^2/2\hbar]$, where $\omega_0 = \sqrt{U''(q_0)/m}$ is the frequency locally defined at q_0 . The ground-state energy is $\hbar\omega_0/2$. These familiar results can be derived from the imaginary-time propagator:

$$K(q_0, q_0; T) = \langle q_0 | e^{-\hat{H}T/\hbar} | q_0 \rangle = \int [\mathcal{D}q(\tau)] e^{-S/\hbar}, \quad (4)$$

where T is the imaginary time duration, \hat{H} is the Hamiltonian of the system,

$$S[q(\tau)] = \int_{-T/2}^{T/2} d\tau \left\{ \frac{m}{2} \left(\frac{dq}{d\tau} \right)^2 + U[q(\tau)] \right\} \quad (5)$$

is the action, and $\int [\mathcal{D}q(\tau)]$ denotes the integration over functions $q(\tau)$ satisfying $q(-T/2) = q(T/2) = q_0$. Note that the imaginary-time (Euclidean) action $S[q(\tau)]$ can be obtained from the real-time (Minkowski) action

$$\mathcal{A}[q(t)] = \int dt \left\{ \frac{m}{2} \left[\frac{dq(t)}{dt} \right]^2 - U[q(t)] \right\}$$

through the formal substitution $t \rightarrow -i\tau$ and $-i\mathcal{A}[q(t)] \rightarrow S[q(\tau)]$. Thus the equation of motion in imaginary time would involve an inverted potential, i.e., $U(q) \rightarrow -U(q)$. An expression for $K(q_0, q_0; T)$ in the limit of $T \rightarrow \infty$ gives both the energy and the wavefunction of the lowest-lying energy eigenstate. In the semiclassical (small \hbar) limit, the functional integral for $K(q_0, q_0; T)$ is dominated by the stationary points of the action, denoted by $\bar{q}(\tau)$, that satisfy the imaginary-time equation of motion

$$\left[\frac{\delta S}{\delta \bar{q}} \right]_{\bar{q}} = -m \frac{d^2 \bar{q}}{d\tau^2} + U'(\bar{q}) = 0,$$

with the boundary condition $\bar{q}(-T/2) = \bar{q}(T/2) = q_0$. There are two solutions: one is $\bar{q}(\tau) = q_0$, at which the Hessian of S , $-m\partial_\tau^2 + U''(q_0)$, has positive eigenvalues only, and the other is the so-called bounce $q_b(\tau)$, at which the Hessian of S , $-m\partial_\tau^2 + U''[q_b(\tau)]$, has a zero eigenvalue plus a negative eigenvalue. The zero eigenvalue comes from the time-translation symmetry and the negative eigenvalue makes $q_b(\tau)$ a saddle point of $S[q(\tau)]$. By following the bounce $q_b(\tau)$ in time, the quantum particle would initially stay at q_0 for a long time, on the order of T , then make a brief excursion to the escape point q_e (separated from q_0 by a potential barrier, with $U(q_e) = U(q_0)$) in a time of order $1/\omega_0$, and finally return to q_0 and remain there for another duration of order T (see Fig. 1b). This process is called a ‘‘bounce’’. Here q_e is the coordinate point at which the quantum tunneling particle leaves the barrier. Physically $q_b(\tau)$ characterizes a fluctuation large enough to accomplish the penetration. [For more details, see Appendix A.] Using the two stationary points of S in the semiclassical approximation with a proper analytic continuation [4], the propagator in Eq. (4) is obtained as

$$|\psi_g(q_0)|^2 e^{-E_g T/\hbar} = (m\omega_0/\pi\hbar)^{1/2} e^{-\omega_0 T/2} e^{-i\text{Im}E_g T/\hbar}, \quad (6)$$

which gives $|\psi_g(q_0)|^2 = (m\omega_0/\pi\hbar)^{1/2}$, the ground-state energy $\hbar\omega_0/2$, and an imaginary part of the energy $\text{Im}E_g$. Physically, $\text{Im}E_g (< 0)$ is responsible for the decay of the metastable “ground state” centered at q_0 , with the decay rate $\Gamma_Q = -2\text{Im}E_g/\hbar$:

$$\Gamma_Q = \omega_0 \sqrt{\frac{S_b}{2\pi\hbar}} \left[\frac{U''(q_0) |\det' \mathcal{H}[q_b(\tau)]|}{\det \mathcal{H}(q_0)} \right]^{-1/2} e^{-S_b/\hbar}, \quad (7)$$

where \mathcal{H} denotes the Hessian of S : $\mathcal{H}[q(\tau)] = -m\partial_\tau^2 + U''[q(\tau)]$, $S_b \equiv S[q_b(\tau)]$ is the action associated with the bounce $q_b(\tau)$, and \det' indicates that the zero eigenvalue is to be omitted in computing the determinant.

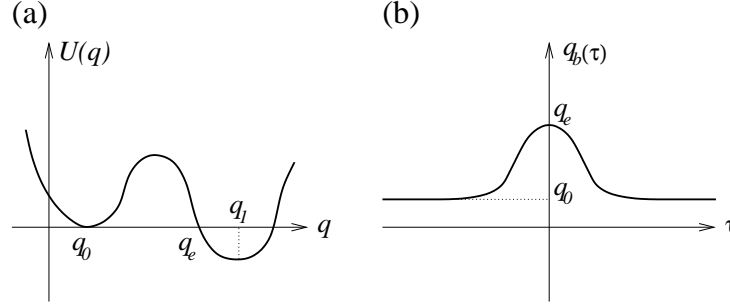


FIG. 1. (a) The potential in one-dimensional space. The unstable ground state is centered at q_0 . After penetrating the barrier, the particle emerges at the escape point q_e and propagates classically. (b) The bounce solution $q_b(\tau)$ for the imaginary-time classical equation of motion. In the inverted potential $-U(q)$, the particle begins at the top of the hill at q_0 , turns around (i.e., bounces) at the classical turning point q_e , and returns to the top of the hill.

C. Numerical implementation of quantum string method

To numerically evaluate Γ_Q , we generalize the string method to the quantum case. For formal similarity, we write the action $S[q(\tau)]$ in Eq. (5) as $S(\mathbf{q})$, where the vector \mathbf{q} represents the coordinates in the $q(\tau)$ -function space (\mathbf{q} space). [Computationally, there are always a large but finite number of these coordinates.] We define the minimal action path (MAP) as a smooth curve $\mathbf{q}^*(s)$ in \mathbf{q} space. It connects the two minima of S , \mathbf{q}_0 and \mathbf{q}_1 , with intrinsic parametrization such as arc length s , satisfying

$$(\nabla S)^\perp(\mathbf{q}^*) = 0, \quad (8)$$

where $(\nabla S)^\perp$ is the component of ∇S normal to the curve $\mathbf{q}^*(s)$. Here \mathbf{q}_0 and \mathbf{q}_1 correspond to $\bar{q}(\tau) = q_0$ and $\bar{q}(\tau) = q_1$, respectively. [A slightly different choice for \mathbf{q}_1 is also possible, corresponding to a $\bar{q}(\tau)$ profile with $\bar{q}(\tau) = q_1$ in most of the τ -interval $[-T/2, T/2]$ and $\bar{q}(-T/2) = \bar{q}(T/2) = q_0$.] The saddle point of S is obtained as the point \mathbf{q}_b which has the maximum value of S along the MAP. This corresponds to the bounce $q_b(\tau)$. To numerically locate the MAP in \mathbf{q} space, a string $\mathbf{q}(s, t)$ connecting \mathbf{q}_0 and \mathbf{q}_1 is evolved according to Eq. (3) with V replaced by S . The stationary solution is the MAP defined by Eq. (8).

The ratio of determinants in Eq. (7) can be numerically obtained as follows:

- (1) From the MAP $\mathbf{q}^*(s)$ parametrized by the arc length s , the eigenvector $\mathbf{u}_b^{(1)}$ corresponding to the negative eigenvalue $\lambda_b^{(1)}$ of the Hessian $\mathcal{H}(\mathbf{q}_b)$ can be obtained by evaluating $d\mathbf{q}^*(s)/ds$ at the saddle point \mathbf{q}_b , followed by a normalization. $\lambda_b^{(1)}$ is then computed from $\lambda_b^{(1)} = [\mathbf{u}_b^{(1)}]^T \mathcal{H}(\mathbf{q}_b) \mathbf{u}_b^{(1)}$.
- (2) The eigenvector $\mathbf{u}_b^{(2)}$ corresponding to the zero eigenvalue $\lambda_b^{(2)}$ of the Hessian $\mathcal{H}(\mathbf{q}_b)$ can be obtained by evaluating $\partial_\tau q_b(\tau)$ from \mathbf{q}_b , followed by a normalization.
- (3) The Hessian $\mathcal{H}(\mathbf{q}_b)$ is modified to give a positive definite matrix $\tilde{\mathcal{H}}(\mathbf{q}_b)$:

$$\tilde{\mathcal{H}}(\mathbf{q}_b) = \mathcal{H}(\mathbf{q}_b) + 2|\lambda_b^{(1)}|[\mathbf{u}_b^{(1)}][\mathbf{u}_b^{(1)}]^T + [\mathbf{u}_b^{(2)}][\mathbf{u}_b^{(2)}]^T, \quad (9)$$

whose determinant $\det \tilde{\mathcal{H}}(\mathbf{q}_b)$ equals $|\det' \mathcal{H}(\mathbf{q}_b)|$.

- (4) In order to compute the ratio of determinants $\det \tilde{\mathcal{H}}(\mathbf{q}_b)/\det \mathcal{H}(\mathbf{q}_0)$, a harmonic potential parametrized by α ($0 \leq \alpha \leq 1$) is constructed as

$$U^\alpha(\mathbf{q}) = \frac{1}{2} \mathbf{q}^T [(1-\alpha)\tilde{\mathcal{H}}(\mathbf{q}_b) + \alpha\mathcal{H}(\mathbf{q}_0)] \mathbf{q} \quad (10)$$

in the N -dimensional \mathbf{q} space. It can be shown [9] that

$$\frac{\det \tilde{\mathcal{H}}(\mathbf{q}_b)}{\det \mathcal{H}(\mathbf{q}_0)} = \exp \left[2 \int_0^1 Q(\alpha) d\alpha \right], \quad (11)$$

where $Q(\alpha)$ is the expectation value

$$Q(\alpha) = \frac{1}{Z(\alpha)} \int d\mathbf{q} \left\{ \frac{1}{2} \mathbf{q}^T [\tilde{\mathcal{H}}(\mathbf{q}_b) - \mathcal{H}(\mathbf{q}_0)] \mathbf{q} \right\} \exp [-U^\alpha(\mathbf{q})], \quad (12)$$

in which $Z(\alpha)$ is the partition function

$$Z(\alpha) = \int d\mathbf{q} \exp [-U^\alpha(\mathbf{q})]. \quad (13)$$

A stochastic process can be generated to measure $Q(\alpha)$ according to Eq. (12) [9].

III. CURRENT-BIASED JOSEPHSON TUNNEL JUNCTION

A. Model formulation

Superconducting devices based on the Josephson effect have been widely used to investigate macroscopic quantum tunneling [16]. We consider the resistively and capacitively shunted junction [12,14,15] for which the classical equation of motion is

$$C \left(\frac{\hbar}{2e} \right)^2 \frac{d^2\phi}{dt^2} + \frac{1}{R} \left(\frac{\hbar}{2e} \right)^2 \frac{d\phi}{dt} + \frac{\partial}{\partial\phi} \left(-\frac{I_c\hbar}{2e} \cos\phi - \frac{I\hbar}{2e} \phi \right) = \frac{\hbar}{2e} I_N(t), \quad (14)$$

where ϕ is the difference in the phases of the order parameters on two sides of the junction, C is the capacitance of the junction, R is the resistance of the junction, I_c is the Josephson critical current, I is the bias current, and $I_N(t)$ is the fluctuating noise current generated by R . Equation (14) is the same as that of a particle of mass $C(\hbar/2e)^2$ moving along the ϕ axis in an effective potential (the so-called “tilted washboard” potential, see Fig. 2)

$$U(\phi) = -\frac{I_c\hbar}{2e} \left[\cos\phi + \frac{I}{I_c}\phi \right].$$

According to this mechanical analog, for $I < I_c$ the zero-voltage state is given by $\phi_0 = \arcsin(I/I_c)$, which is a minimum of $U(\phi)$. In the classical limit, the escape from the zero-voltage state is induced by the noise current which activates the system over the potential barrier [12]. At sufficiently low temperatures, although thermodynamic fluctuations are suppressed, the junction can still escape from the zero-voltage state through quantum barrier tunneling [14,15].

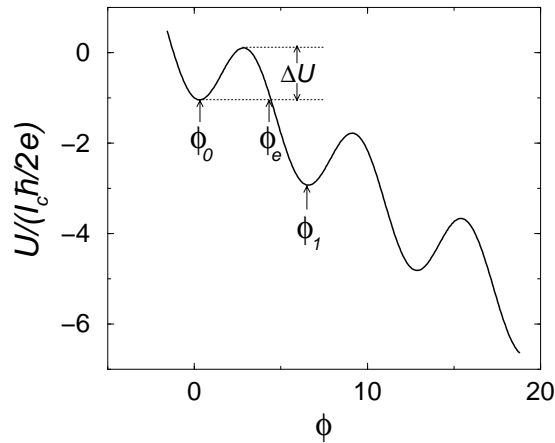


FIG. 2. The tilted washboard potential $U(\phi)$ for $I/I_c = 0.3$. Here the unstable ground state is centered at ϕ_0 , ϕ_e is the escape point, and $\phi_1 = \phi_0 + 2\pi$ is the next minimum.

We consider the zero-temperature behavior of the junction in the low-damping limit $((2eI_c/\hbar C)^{1/2}[1 - (I/I_c)^2]^{1/4}RC \gg 1)$. The state of the junction is represented by the wave function $\Psi(\phi, t)$, governed by the Schrödinger equation $i\hbar\partial\Psi/\partial t = \hat{H}\Psi$ in which the Hamiltonian is of the form

$$\hat{H} = -\frac{(2e)^2}{2C} \frac{\partial^2}{\partial\phi^2} + U(\phi).$$

We introduce three parameters: the dimensionless bias current $x = I/I_c$, the plasma frequency $\omega_p = \sqrt{2eI_c/\hbar C}$, and $I_c/2e\omega_p = \sqrt{E_J/E_C}$ where $E_J = I_c\hbar/2e$ is the Josephson coupling energy and $E_C = (2e)^2/C$ is the charging energy. The imaginary-time action

$$S[\phi(\tau)] = \int d\tau \left[\frac{1}{2}C \left(\frac{\hbar}{2e} \right)^2 \left(\frac{d\phi}{d\tau} \right)^2 + U(\phi) \right], \quad (15)$$

can be written as $S[\phi(\tau)] = \hbar\sqrt{E_J/E_C}\bar{S}[\phi(\bar{\tau})]$, where $\bar{\tau} = \omega_p\tau$ is a dimensionless time variable and \bar{S} is the dimensionless action

$$\bar{S}[\phi(\bar{\tau})] = \int d\bar{\tau} \left[\frac{1}{2} \left(\frac{d\phi}{d\bar{\tau}} \right)^2 + (-\cos\phi - x\phi) \right]. \quad (16)$$

B. Numerical results

Based on the actions (15) and (16), the tunneling rate is given by

$$\Gamma_Q = \omega_p \sqrt{\cos\phi_0} \left(\frac{E_J}{E_C} \right)^{1/4} \sqrt{\frac{\bar{S}_b}{2\pi}} \left[\frac{\cos\phi_0 |\det' \mathcal{H}[\phi_b(\bar{\tau})]|}{\det \mathcal{H}(\phi_0)} \right]^{-1/2} \exp \left(-\sqrt{\frac{E_J}{E_C}} \bar{S}_b \right), \quad (17)$$

according to the general expression (7). Here $\omega_p\sqrt{\cos\phi_0}$ is the frequency locally defined at ϕ_0 , $\bar{S}_b \equiv \bar{S}[\phi_b(\bar{\tau})]$ is the dimensionless action of the bounce $\phi_b(\bar{\tau})$ which satisfies $\phi_b(\pm\infty) = \phi_0$, and \mathcal{H} is the Hessian of $\bar{S}[\phi(\bar{\tau})]$, given by $\mathcal{H}[\phi(\bar{\tau})] = -\partial^2/\partial\bar{\tau}^2 + \cos[\phi(\bar{\tau})]$. Numerical calculations based on the action in Eq. (16) have been carried out to evaluate the bounce $\phi_b(\bar{\tau})$, the bounce action \bar{S}_b , and the ratio of determinants in the general expression (17). Note that these dimensionless properties are uniquely determined by the parameter x . Once they are evaluated, the tunneling rate Γ_Q can be readily obtained using the other two parameters ω_p and $\sqrt{E_J/E_C}$. These parameters should be easily measurable experimentally, since they are directly determined from the capacitance of the junction, the critical current, and the bias current.

Numerical calculations have been carried out according to the following procedure.

(i) We first locate the MAP in the $\phi(\bar{\tau})$ -function space. In the calculation, $\phi(\bar{\tau})$ is represented by a column vector $\boldsymbol{\phi}$ of $N = 200$ entries, with the $\bar{\tau}$ -interval $[-\bar{T}/2, \bar{T}/2]$ discretized by a uniform mesh of N points. We use $\bar{T} = 20$, large enough for the computation of zero-temperature properties. [Here $\bar{T} = \hbar\omega_p/k_B\mathcal{T}$, where k_B is the Boltzmann constant and \mathcal{T} the temperature, and $\bar{T} \gg 1$ means $\hbar\omega_p \gg k_B\mathcal{T}$.] The string $\boldsymbol{\phi}(s)$ connecting $\boldsymbol{\phi}(0) = \boldsymbol{\phi}_0$ and $\boldsymbol{\phi}(1) = \boldsymbol{\phi}_1$ is discretized by $M = 200$ points in the $\boldsymbol{\phi}$ space. As to the two fixed ends of the string, $\boldsymbol{\phi}_0$ corresponds to $\phi(\bar{\tau}) = \phi_0$ and $\boldsymbol{\phi}_1$ to a $\phi(\bar{\tau})$ profile with $\phi(\bar{\tau}) = \phi_1$ in most of the $\bar{\tau}$ -interval and $\phi(-\bar{T}/2) = \phi(\bar{T}/2) = \phi_0$. Here $\phi_0 = \arcsin x$ and $\phi_1 = \phi_0 + 2\pi$ are two neighboring minima of $-(\cos\phi + x\phi)$ (see Fig. 2). Note that $\boldsymbol{\phi}_1$ is obtained as a local minimum of \bar{S} in Eq. (16). The string evolution is generated by

$$(d\boldsymbol{\phi}/ds)^\perp = -(\nabla\bar{S})^\perp(\boldsymbol{\phi}),$$

with the initial string taken from a linear interpolation between $\boldsymbol{\phi}_0$ and $\boldsymbol{\phi}_1$. The MAP $\boldsymbol{\phi}^*(s)$ is reached by the evolving string $\boldsymbol{\phi}(s, t)$ as its stationary solution defined by $(\nabla\bar{S})^\perp(\boldsymbol{\phi}^*) = 0$, with $\boldsymbol{\phi}^*(0) = \boldsymbol{\phi}_0$ and $\boldsymbol{\phi}^*(1) = \boldsymbol{\phi}_1$. The bounce $\phi_b(\bar{\tau})$ is obtained from the vector $\boldsymbol{\phi}_b$ which yields the maximum value of \bar{S} along the MAP. In Fig. 3 a sequence of the $\phi(\bar{\tau})$ profiles along the MAP is shown for $x = 0.1$, and in Fig. 4 the bounce profile $\phi_b(\bar{\tau})$ is shown for a few selected values of x . In Fig. 5 the variation of the action \bar{S} along the MAP is shown for a few selected values of x , and in Fig. 6 the bounce action \bar{S}_b is plotted as a function of x .

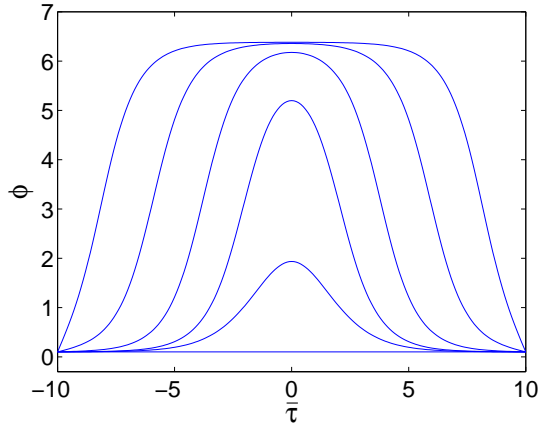


FIG. 3. A sequence of the $\phi(\bar{\tau})$ profiles along the MAP for $x = 0.1$. From bottom to top, the first curve denotes $\phi(\bar{\tau}) = \phi_0$ which is a local minimum of $\bar{S}[\phi(\bar{\tau})]$, the third curve denotes the bounce $\phi_b(\bar{\tau})$, and the last curve denotes another local minimum of $\bar{S}[\phi(\bar{\tau})]$ with $\phi(0) = \phi_1$ and $\phi(-\bar{T}/2) = \phi(\bar{T}/2) = \phi_0$.

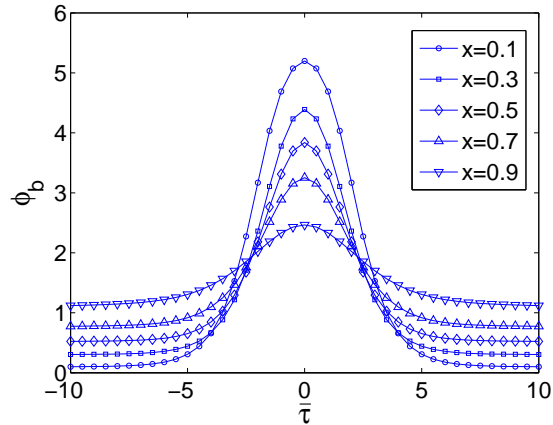


FIG. 4. The bounce $\phi_b(\bar{\tau})$, plotted for a few selected values of x .

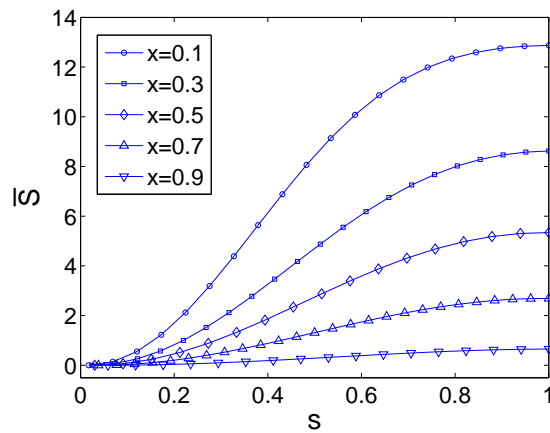


FIG. 5. The dimensionless action along a segment of the MAP starting from $\phi(\bar{\tau}) = \phi_0$ and ending at $\phi_b(\bar{\tau})$. Here \bar{S} is plotted as a function of the arc length s in the $\phi(\bar{\tau})$ -function space for a few selected values of x . The profile of $\phi(\bar{\tau}) = \phi_0$ is taken as the reference point $s = 0$ at which \bar{S} has been set to be zero by a constant shift of the potential.

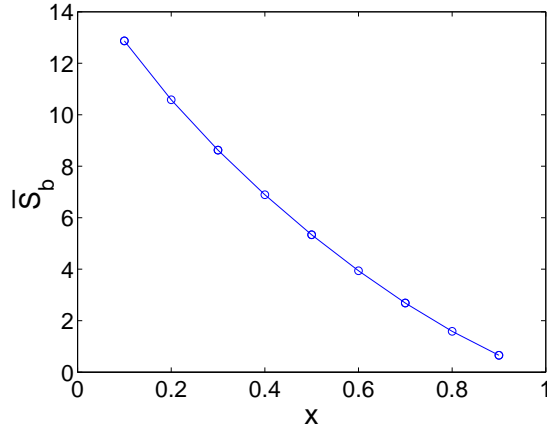


FIG. 6. The bounce action \bar{S}_b plotted as a function of x .

(ii) We then modify the Hessian $\mathcal{H}[\phi_b(\bar{\tau})]$, represented by the $N \times N$ matrix $\mathcal{H}(\phi_b)$, to give a positive definite matrix $\tilde{\mathcal{H}}(\phi_b)$, given by

$$\tilde{\mathcal{H}}(\phi_b) = \mathcal{H}(\phi_b) + 2|\lambda_b^{(1)}|[\mathbf{u}_b^{(1)}][\mathbf{u}_b^{(1)}]^T + \cos \phi_0[\mathbf{u}_b^{(2)}][\mathbf{u}_b^{(2)}]^T.$$

Here $\mathbf{u}_b^{(1)}$ is the eigenvector corresponding to the negative eigenvalue $\lambda_b^{(1)}$ of the Hessian $\mathcal{H}(\phi_b)$, $\mathbf{u}_b^{(2)}$ is the eigenvector corresponding to the zero eigenvalue $\lambda_b^{(2)}$ of the same Hessian, and $\det \tilde{\mathcal{H}}(\phi_b) = \cos \phi_0 |\det' \mathcal{H}(\phi_b)|$. Note that $\mathbf{u}_b^{(1)}$, $\lambda_b^{(1)}$, and $\mathbf{u}_b^{(2)}$ can be readily obtained once the MAP is determined, as outlined in Sec. II C. In Fig. 7 the unstable direction $\mathbf{u}_b^{(1)}$ along the MAP at the saddle point is shown for a few selected values of x .

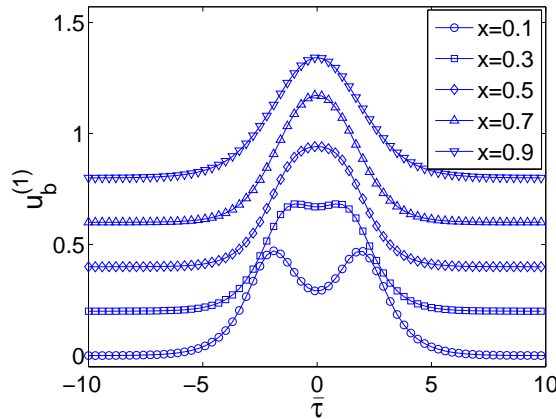


FIG. 7. The eigenfunction $u_b^{(1)}(\bar{\tau})$ of the Hessian $\mathcal{H}[\phi_b(\bar{\tau})]$ with the negative eigenvalue, plotted for a few selected values of x . The curves are displaced vertically for clarity, whereas the original ones all start and end at 0. Each eigenfunction represents the unstable direction at the saddle point along a particular MAP in the $\phi(\bar{\tau})$ -function space. It is noted that $u_b^{(1)}(\bar{\tau})$ obtained for $x = 0.1$ is qualitatively different from that for $x = 0.9$. For x close to 0, the bounce $\phi_b(\bar{\tau})$ has the height ϕ_e (the escape point) close to the next (lower) minimum ϕ_1 , and the growth of the $\phi(\bar{\tau})$ bubble along the MAP is characterized by the movement of the two (left and right) domain walls. Consequently, the unstable direction $u_b^{(1)}(\bar{\tau})$ shows two peaks. On the other hand, for $x > 0.3$, the bounce $\phi_b(\bar{\tau})$ has the height ϕ_e far from the next minimum ϕ_1 , and the growth of the $\phi(\bar{\tau})$ bubble along the MAP is characterized by overall dilation. Consequently, the unstable direction $u_b^{(1)}(\bar{\tau})$ displays one peak only.

(iii) We calculate the ratio of determinants

$$\gamma = \frac{\cos \phi_0 |\det' \mathcal{H}[\phi_b(\bar{\tau})]|}{\det \mathcal{H}(\phi_0)} = \frac{\cos \phi_0 |\det' \mathcal{H}(\phi_b)|}{\det \mathcal{H}(\phi_0)}, \quad (18)$$

where $\mathcal{H}(\phi_0)$ is the $N \times N$ matrix representation of $\mathcal{H}(\phi_0)$. This is done by evaluating $\det \tilde{\mathcal{H}}(\phi_b)/\det \mathcal{H}(\phi_0)$ according to the stochastic method outlined in Sec. II C. Numerical results of this part are shown in Figs. 8 and 9, for the stochastically measured $Q(\alpha)$ in Eqs. (11) and (12) and the ratio of determinants γ in Eq. (18). From \bar{S}_b and γ , the dimensionless prefactor $\sqrt{\cos \phi_0} \sqrt{\frac{\bar{S}_b}{2\pi}} \left[\frac{\cos \phi_0 |\det' \mathcal{H}[\phi_b(\bar{\tau})]|}{\det \mathcal{H}(\phi_0)} \right]^{-1/2}$ in Eq. (17) is readily obtained and plotted in Fig. 10.

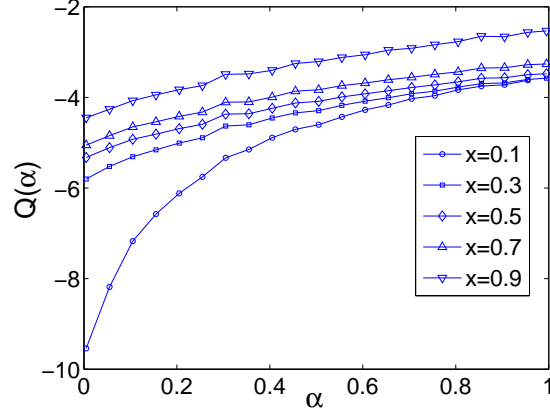


FIG. 8. Stochastically measured $Q(\alpha)$, plotted for a few selected values of x .

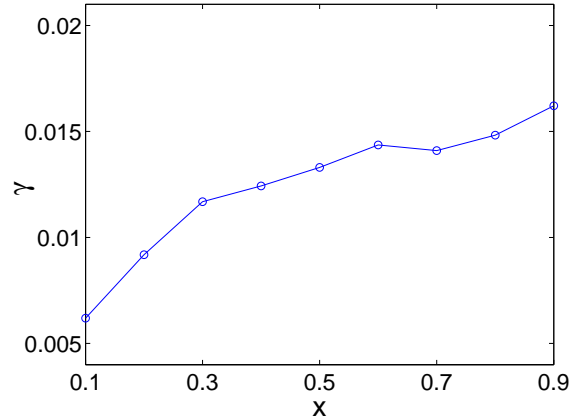


FIG. 9. The determinant ratio γ in Eq. (18) plotted as a function of x .

Using the numerical results for \bar{S}_b and γ , the mean escape rate out of the zero-voltage state can be readily obtained from Eq. (17), once the values of ω_p and $\sqrt{E_J/E_C}$ are given. From $I_c = 9.489 \mu\text{A}$ and $C = 6.35 \text{ pF}$ reported in an early experiment [15], we have $\omega_p = 67.4 \text{ GHz}$ and $\sqrt{E_J/E_C} = 440$. The largeness of $\sqrt{E_J/E_C}$ implies that quantum tunneling becomes observable only if $x \rightarrow 1$ and $\bar{S}_b \rightarrow 0$. For the experiment reported in Ref. [15], $x \approx 0.99$ at which $\bar{S}_b \approx 0.037$, $e^{-\sqrt{E_J/E_C}\bar{S}_b} \sim 10^{-7}$, and the escape rate is approximately $2.7 \times 10^4 \text{ sec}^{-1}$. In a recent experiment on quantum superposition of macroscopic persistent-current states, a superconducting loop is constructed with three Josephson junctions [21]. We find that the junction parameters in that experiment allow quantum tunneling to be observable in a range of x much wider than that in Ref. [15]. From $I_c = 570 \text{ nA}$ and $C = 2.6 \text{ fF}$ [21], we have $\omega_p = 816 \text{ GHz}$ and $\sqrt{E_J/E_C} = 2.18$. The smallness of $\sqrt{E_J/E_C}$ then allows \bar{S}_b and hence x to vary in a wide range. For x decreasing from 0.8 to 0.2, \bar{S}_b roughly increases from 2 to 10, and consequently, $e^{-\sqrt{E_J/E_C}\bar{S}_b}$ changes from $\sim 10^{-2}$ to $\sim 10^{-10}$. Using Eq. (17) with the numerical results for \bar{S}_b and γ , we obtain the escape rates $\Gamma_Q = 1.2 \times 10^{11} \text{ sec}^{-1}$, $7.4 \times 10^7 \text{ sec}^{-1}$, and $1.5 \times 10^3 \text{ sec}^{-1}$, for $x = 0.8, 0.5$, and 0.2 , respectively. Note that typically,

the measured escape rates are in the range from $\sim 10^1$ to $\sim 10^6$ sec^{-1} . Therefore, our numerical results indicate that the absolute escape rates for today's nanojunctions should be measurable at bias current much below the critical current. This is because the junction capacitance has been significantly reduced and thus the action scale $\sqrt{E_J/E_C}$ can be made small enough to allow a relatively large dimensionless action \bar{S}_b in the exponential factor $e^{-\sqrt{E_J/E_C}\bar{S}_b}$ [22]. In this regard a numerical scheme as presented in this paper is essential to the evaluation of the absolute escape rates.

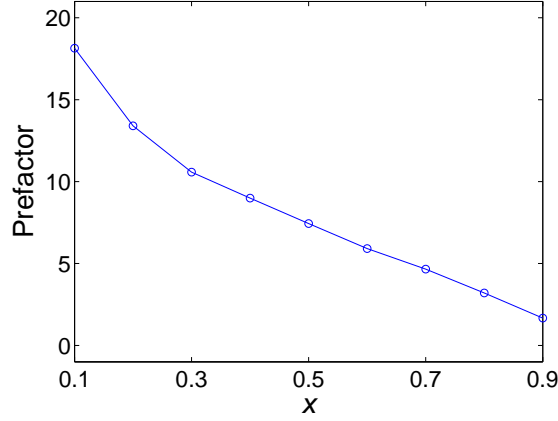


FIG. 10. The dimensionless prefactor $\sqrt{\cos \phi_0} \sqrt{\frac{\bar{S}_b}{2\pi}} \left[\frac{\cos \phi_0 |\det' \mathcal{H}[\phi_b(\bar{\tau})]|}{\det \mathcal{H}(\phi_0)} \right]^{-1/2}$ in Eq. (17), plotted as a function of x . Note the large variation of a factor > 10 as a function of x .

C. Quadratic-plus-cubic potential

For bias currents less than but very close to I_c (x close to 1), the potential barrier ΔU to be penetrated is low, the distance between the minimum ϕ_0 and the escape point ϕ_e is small, and hence the potential $U(\phi)$ in the classically forbidden region can be approximated by the quadratic-plus-cubic potential. That is, the dimensionless potential $-\cos \phi - x\phi$ in the action (16) can be expressed in a Taylor expansion form

$$u(\phi) = -\cos \phi - x\phi \approx (-\cos \phi_0 - x\phi_0) + \frac{1}{2} \cos \phi_0 (\phi - \phi_0)^2 \left(1 - \frac{\phi - \phi_0}{\phi_e - \phi_0} \right), \quad (19)$$

where $\phi_e - \phi_0 = 3 \cot \phi_0$ approaches zero as $x \rightarrow 1$ and $\phi_0 \rightarrow \pi/2$. From Eq. (19), the dimensionless potential barrier can be easily found to be $\Delta u = 2 \cos \phi_0 (\phi_e - \phi_0)^2 / 27$ and the dimensionless bounce action to be $\bar{S}_b = 8 \sqrt{\cos \phi_0} (\phi_e - \phi_0)^2 / 15$. In addition, the Hessian of $\bar{S}[\phi(\bar{\tau})]$ becomes $\mathcal{H}[\phi(\bar{\tau})] = -\partial^2 / \partial \bar{\tau}^2 + \cos \phi_0 [1 - 3(\phi - \phi_0) / (\phi_e - \phi_0)]$, for which the analytic result

$$\frac{\cos \phi_0 |\det' \mathcal{H}[\phi_b(\bar{\tau})]|}{\det \mathcal{H}(\phi_0)} = \frac{1}{60}$$

has been obtained for the determinant ratio γ in Eq. (18) [17,18]. These exact results for the quadratic-plus-cubic potential allow an analytic form for the tunneling rate Γ_Q in Eq. (7). Numerical results for $x = 0.9$ in Figs. 6 and 9 show that $\frac{\bar{S}_b}{\sqrt{\cos \phi_0} (\phi_e - \phi_0)^2} = 0.469$, approaching $8/15$, and the determinant ratio $\gamma = 0.0162$, approaching $1/60$, though $\phi_e - \phi_0 = 1.45$ is still large.

In order to demonstrate the validity and precision of the quantum string method, numerical calculations have been carried out to reproduce the bounce action and determinant ratio for the quadratic-plus-cubic potential, an important model potential for the study of quantum metastability [18]. For simplicity, we work with the scaled action functional

$$S[q(\tau)] = \int d\tau \left[\frac{1}{2} \left(\frac{dq}{d\tau} \right)^2 + \frac{1}{2} q^2 (1 - q) \right]. \quad (20)$$

The potential $q^2(1-q)/2$ in action (20) has $q_0 = 0$ as the metastable minimum and $q_e = 1$ as the escape point. For computational purpose, this potential is distorted in the region of $q \gg q_e$ to generate another (lower) minimum at $q_1 (\gg q_e)$. Numerically, the two potential minima q_0 and q_1 are used to fix the ends of the evolving string in the $q(\tau)$ -function space. The stationary solution for the string evolution equation is the MAP from which the saddle point of $S[q(\tau)]$, i.e., the bounce $q_b(\tau)$, can be obtained. Since the potential profile is untouched in the classically forbidden region ($q_0 \leq q \leq q_e$), the bounce so obtained is not affected by the potential distortion far away. The bounce action $S_b \equiv S[q_b(\tau)]$ is obtained to be 0.5337, very close to the exact result 8/15. The determinant ratio

$$\frac{|\det' \mathcal{H}[q_b(\tau)]|}{\det \mathcal{H}(q_0)} = \frac{|\det' [-\partial^2/\partial\tau^2 + 1 - 3q_b(\tau)]|}{\det(-\partial^2/\partial\tau^2 + 1)} \left(= \frac{1}{60} \right) \quad (21)$$

is obtained to be 0.0142, close to 1/60. These results are obtained for $N = 200$, $M = 200$, and the total imaginary time duration $T = 20$. Better agreement with the exact results can certainly be achieved by using longer imaginary time duration, vector space of higher dimensionality, and finer resolution in discretizing the string.

IV. CONCLUDING REMARKS

Quantum tunneling in macroscopic systems is intimately related to the important issue of quantum dissipation, which arises from the coupling to environmental variables. This coupling can modify the tunneling itself, as many prior works have shown [5,17,23,24]. However, it should be noted that regardless of the particulars in the quantum dissipation model, the net result is to decrease the escape rate. Hence the rate calculated for nondissipative quantum tunneling may be regarded as an upper bound to the rate(s) with nonzero dissipation.

In this regard it should also be noted that as a tool for the numerical evaluation of tunneling rate in the path integral formalism, the quantum string method is directly generalizable to field theoretic problems, requiring only additional computational resources.

ACKNOWLEDGMENTS

T. Q. was supported by the Hong Kong RGC under grant 602805. J. S. and W. E. were supported by DOE under grant DE-FG02-03ER25587. P. S. was supported by the Hong Kong RGC under grants HKUST6073/02P and CA04/05.SC02.

APPENDIX A: THE BOUNCE

The bounce $q_b(\tau)$ is a solution of the imaginary-time classical equation of motion:

$$m \frac{d^2 \bar{q}}{d\tau^2} = U'(\bar{q}),$$

subject to the boundary condition $\bar{q}(-T/2) = \bar{q}(T/2) = q_0$ for $T \rightarrow \infty$. The qualitative behavior of $q_b(\tau)$ is suggested by the analogy with the equation of motion for a particle of mass m in the inverted potential $-U(q)$, in which q_0 now corresponds to the top of the hill and q_e to the classical turning point. The particle would spend most of its time at q_0 (due to zero velocity), but, in the course of an arbitrarily long interval of time, it would make a brief excursion to the point q_e and then return to q_0 (see Fig. 1b). Note that

$$\frac{m}{2} \left(\frac{d\bar{q}}{d\tau} \right)^2 - U[\bar{q}(\tau)] = -U(q_0) = 0$$

is a constant of motion for $q_b(\tau)$. This means $dq_b/d\tau$ vanishes at q_0 and q_e .

The bounce $q_b(\tau)$ shown in Fig. 1b is centered at $\tau_c = 0$ along the τ axis. Because of the time-translation invariance of the action, the bounce solutions are also given by $q_b(\tau - \tau_c)$, where τ_c is an arbitrary center of the bounce. This symmetry property leads to a zero eigenvalue for the Hessian of S at $q_b(\tau)$, $-m\partial_\tau^2 + U''[q_b(\tau)]$. The corresponding eigenfunction is given by

$$u_b^{(2)}(\tau) = \sqrt{\frac{m}{S_b}} \frac{dq_b}{d\tau},$$

where $\sqrt{m/S_b}$ is the normalization factor derived from the action of the bounce,

$$S_b = \int_{-T/2}^{T/2} d\tau \left\{ \frac{m}{2} \left(\frac{dq_b}{d\tau} \right)^2 + U[q_b(\tau)] \right\},$$

and the constant of motion

$$\frac{m}{2} \left(\frac{dq_b}{d\tau} \right)^2 - U[q_b(\tau)] = 0.$$

Note that $dq_b/d\tau$ has a zero at the center of the bounce. Therefore, $u_b^{(2)}(\tau)$ has a node and can not be the eigenfunction with the lowest eigenvalue: there must be a nodeless eigenfunction, $u_b^{(1)}(\tau)$, with a negative eigenvalue. This implies that the bounce is not a minimum of the action but a saddle point. The negative eigenvalue requires a proper analytical continuation in evaluating the functional integral in (4). This leads to a complex energy in (6).

Using the constant of motion, the bounce action can be reduced to the form

$$S_b = \int_{-T/2}^{T/2} m \left(\frac{dq_b}{d\tau} \right)^2 d\tau = 2 \int_{q_0}^{q_e} \sqrt{2mU(q)} dq.$$

It is seen that $e^{-S_b/2\hbar}$ is the familiar WKB exponential factor for the amplitude of tunneling wave. Accordingly, $e^{-S_b/\hbar}$ is the exponential factor for the current density of the tunneling wave, which is directly related to the rate of decay. This is reflected in Eq. (7). We want to remark that for one-dimensional quantum mechanics, the tunneling rate (7) derived from functional integral agrees with that obtained by standard WKB method of wave mechanics [4].

- [1] H. A. Kramers, *Physica* **7**, 284 (1940).
- [2] R. Landauer and J. A. Swanson, *Phys. Rev.* **121**, 1668 (1961).
- [3] J. S. Langer, *Ann. Phys. (N.Y.)* **41**, 108 (1967); J. S. Langer, *Phys. Rev. Lett.* **21**, 973 (1968).
- [4] S. Coleman, *Phys. Rev. D* **15**, 2929 (1977); C. G. Callan, Jr. and S. Coleman, *Phys. Rev. D* **16**, 1762 (1977).
- [5] A. O. Caldeira and A. J. Leggett, *Phys. Rev. Lett.* **46**, 211 (1981).
- [6] I. Affleck, *Phys. Rev. Lett.* **46**, 388 (1981).
- [7] W. E, W. Ren, and E. Vanden-Eijnden, *Phys. Rev. B* **66**, 052301 (2002).
- [8] W. E, W. Ren, and E. Vanden-Eijnden, *J. Appl. Phys.* **93**, 2275 (2003).
- [9] W. E, W. Ren, and E. Vanden-Eijnden, *Zero-temperature string method for the study of rare events*, unpublished.
- [10] W. Ren, *Comm. Math. Sci.* **1**, 377 (2003).
- [11] T. Qian, W. Ren, and P. Sheng, *Phys. Rev. B* **72**, 014512 (2005).
- [12] V. Ambegaokar and B. I. Halperin, *Phys. Rev. Lett.* **22**, 1364 (1969).
- [13] T. A. Fulton and L. N. Dunkleberger, *Phys. Rev. B* **9**, 4760 (1974).
- [14] R. F. Voss and R. A. Webb, *Phys. Rev. Lett.* **47**, 265 (1981).
- [15] J. M. Martinis, M. H. Devoret, and J. Clarke, *Phys. Rev. B* **35**, 4682 (1987).
- [16] A. J. Leggett, *Prog. Theor. Phys. (Suppl.)* **69**, 80 (1980); A. J. Leggett, *J. Phys.: Condens. Matter* **14**, R415 (2002).
- [17] A. O. Caldeira and A. J. Leggett, *Ann. Phys. (N.Y.)* **149**, 374 (1983).
- [18] M. Ueda and A. J. Leggett, *Phys. Rev. Lett.* **80**, 1576 (1998).
- [19] J. S. Langer and V. Ambegaokar, *Phys. Rev.* **164**, 498 (1967).
- [20] D. E. McCumber and B. I. Halperin, *Phys. Rev. B* **1**, 1054 (1970).
- [21] C. H. van der Wal *et al.*, *Science* **290**, 773 (2000).
- [22] The scale of the imaginary-time action, $\sqrt{E_J/E_C}$, can be written as $E_J/\hbar\omega_p$. For small bias current $I \ll I_c$ ($x \ll 1$), the ground-state energy ($\approx \hbar\omega_p/2$) must be small compared to the barrier height ΔU ($\approx 2E_J$). Otherwise, the system loses metastability. For $\sqrt{E_J/E_C} = 2.18$ in our calculations, the barrier height is about 9 times the ground-state energy and metastability can be safely assumed. Further reduction of the junction capacitance would eventually destroy this metastability.
- [23] E. Freidkin, P. S. Riseborough, and P. Hänggi, *Z. Phys. B* **64**, 237 (1986).
- [24] U. Weiss, *Quantum Dissipative Systems* (World Scientific, Singapore, 1993).